Photo-ionization of the helium atom close to the double ionization threshold: towards the Ericson regime

Benoît Grémaud and Dominique Delande
Laboratoire Kastler-Brossel, Université Pierre et Marie Curie, 4 Place Jussieu, 75005 Paris, France
(February 5, 2008)

We calculate the photo-ionization cross-section from the ground state of the helium atom, using the complex rotation method and diagonalization of sparse matrices. This produces directly the positions and widths of the doubly excited $^1\mathbf{P}^o$ resonances together with the photo-ionization cross-section. Our calculations up to the $N = 9$ threshold are in perfect agreement with recent experimental data and show the transition from a regular structure at low energy to a chaotic one at high energy, where various resonances strongly overlap.

The Helium atom is one of the prototype of atomic systems whose classical dynamics is mainly chaotic and during the past thirty years, it has been matter of numerous studies from both theoretical [1–8] and experimental [9,10,12] points of view. But, unlike other atomic systems like for instance the hydrogen atom in magnetic field, the effects of chaos are not very well understood and more profound studies are needed. This requires the resolution of the full quantum problem. Especially, one has to take into account all the degrees of freedom and all correlations between the two electrons, as well as the auto-ionizing character of the doubly excited states.

In this letter, we present numerical calculations of the cross-section of the one-photon photoionization from the ground state of the helium atom and compare them with the recently obtained high-resolution spectra of $^1\mathbf{P}^o$ doubly excited states. The agreement with the most recent experimental data from references [10,12] – up to the $N = 9$ ionization threshold, less than 1 eV from the double ionization threshold and corresponding to 64 open channels – is excellent for the whole energy range, proving the high efficiency of the method. Predictions for better experimental resolutions are also given. We also show that at low energy the resonances can be classified with respect to the Herrick's (N, K, T) approximate quantum numbers [2], ($(N, K)_n$ Lin's simplified notation [3] will be used hereafter). At high energy, this classification progressively breaks down. Eventually, above the $N = 7$ threshold, the various resonances strongly overlap: the mean energy spacing between consecutive resonances becomes smaller than their typical width. Oscillations in the photo-ionization cross-section can then no longer be associated with individual resonances: random-like fluctuations – known as Ericson fluctuations – should be observed in the cross-section.

The quantum Hamiltonian in atomic units ($\hbar = m_{e^-} = 4\pi\epsilon_0 = e^2 = 1$) is given by:

$$H = \frac{\mathbf{P}_1^2 + \mathbf{P}_2^2}{2} - \frac{2}{r_1} - \frac{2}{r_2} + \frac{1}{r_{12}} \tag{1}$$

where $\mathbf{P}_i = -\imath\hbar\nabla_i$ is the momentum operator of electron i, r_i its distance to the nucleus and r_{12} the inter-electronic distance. All spin-orbits, relativistic and QED effects (at most of the order of a fraction of meV) are neglected, which is consistent with the experimental resolution (of the order of 1 meV). The corrections due the finite mass of the nucleus are taken into account by using the effective values for the double-ionization threshold I_∞ and the Rydberg constant R_{He} given in the reference [10], namely $I_\infty = 79.003$ eV and $R_{He} = 13.6038$ eV.

Using the rotational invariance of the Hamiltonian, the angular dependency of a wavefunction can be factorized as follows [11]:

$$\Psi_{L\,M} = \sum_{T=-L}^{L} \mathcal{D}^{L\,*}_{MT}(\psi, \theta, \phi)\Phi_T^{(LM)}(x, y, z) \tag{2}$$

where (ψ, θ, ϕ) are Euler angles defining the transformation from the laboratory frame to a molecular-like frame whose z' axis is the inter-electronic axis. $|T|$ is then the Λ (Σ, Π...) quantum number in a molecule. The $\mathcal{D}^{L\,*}_{MT}$ are the wavefunctions of the rigid rotor and reduce to the usual spherical harmonics for $T = 0$. Finally (x, y, z) are the perimetric coordinates, symmetric combinations of r_1, r_2 and r_{12}:

$$\begin{cases} x = & r_1 + r_2 - r_{12} \\ y = & r_1 - r_2 + r_{12} \\ z = & -r_1 + r_2 + r_{12} \end{cases} \tag{3}$$

For each pair of good quantum numbers (L, M), we obtain an effective Hamiltonian acting on the different Φ_T's (coupled by Coriolis-like terms). The two remaining discrete symmetries – parity and exchange between the two electrons – are exactly taken into account by adding constraints on the Φ_T's [8].

As stated before, above the first ionization threshold, all states become resonances because of the coupling with the continua (autoionizing states). Using the complex rotation method [5,13], we obtain these resonances as complex eigenvalues of a complex Hamiltonian $H(\theta)$, which is obtained by the replacements $\mathbf{r}_i \to \mathbf{r}_i e^{\imath\theta}$ and $\mathbf{P}_i \to \mathbf{P}_i e^{-\imath\theta}$, where θ is a real parameter. The fundamental properties of the spectrum of $H(\theta)$ are the following : the continua of H are rotated by an angle 2θ in the lower complex half-plane around their branching point. Each other complex eigenvalue $E_i = \epsilon_i - i\Gamma_i/2$ lies in the lower half-plane and coincides with a resonance of H with energy ϵ_i and width Γ_i. These quantities are independent of θ provided that the complex eigenvalue has been uncovered by the rotated continua. The bound states, which are resonances with zero width, stay on the real axis. This method also allows to compute quantities of physical interest, like photo-ionization cross-section, probability densities or expectation values of operators (e.g. $\cos\theta_{12}$), enlighting the contribution of a given resonance to them. For instance, the cross-section is given by [13] :

$$\sigma(\omega) = \frac{4\pi\omega}{c}\mathrm{Im}\sum_i \frac{\langle\overline{E_{i\theta}}|R(\theta)T|g\rangle^2}{E_{i\theta} - E_g - \hbar\omega} \tag{4}$$

T is the dipole operator, $\hbar\omega$ is the photon energy, $|g\rangle$ is the ground state (of energy E_g). $\langle\overline{E_{i\theta}}|$ is the transpose of the eigenvector $|E_{i\theta}\rangle$ of $H(\theta)$ for the eigenvalue $E_{i\theta}$ (i.e. the complex conjugate of $\langle E_{i\theta}|$). $R(\theta)$ is the rotation operator, essential to obtain the right (complex) oscillator strength.

In the preceding formula, each eigenvalue (resonance or continuum) contributes to the cross-section at energy $\hbar\omega + E_g$, with a Fano profile centered at energy $\mathrm{Re}E_i$, of width $-2\mathrm{Im}E_i$ whose q parameter is given by [13]:

$$q = -\frac{\mathrm{Re}\langle\overline{E_{i\theta}}|R(\theta)T|g\rangle}{\mathrm{Im}\langle\overline{E_{i\theta}}|R(\theta)T|g\rangle} \tag{5}$$

Thus, the Fano-q parameter of one resonance is directly and unambiguously obtained from its associated eigenvector, which is much more efficient than any fitting procedure, especially above the $N = 6$ threshold where the different series strongly overlap (see fig. 1).

For an efficient numerical resolution, the effective Hamiltonian is expanded in the product of three Sturmian-like basis $|n_x\rangle \otimes |n_y\rangle \otimes |n_z\rangle$, one for each perimetric coordinate. The basis states have the following expression:

$$\text{with} \quad \langle u|n\rangle = \phi_n(u) = \sqrt{\alpha_u} L_n(\alpha_u u) e^{-\alpha_u \frac{u}{2}} \tag{6}$$

where $n_{x,y,z}$ are non negative integers, $\alpha_{x,y,z}$ are real positive parameters (the scaling parameters) and L_n the n^{th} Laguerre polynomial. This non-orthogonal basis is associated with a representation of the dynamical group SO(2,1), which gives rise to selection rules. The matrix representation of the effective Hamiltonian in this basis is thus sparse and banded, and the matrix elements are analytically known. Let us emphasize that this approach is "exact" for the non-relativistic *He* atom and similar to the one used in reference [8].

For obvious reasons, the basis has to be truncated, the prescription being $n_x + n_y + n_z \leq N_{\max}$ (we used up to $N_{\max} = 58$). The different scaling parameters are related by $\alpha = \alpha_x = 2\alpha_y = 2\alpha_z$, which increases the sparsity of the matrices and gives the correct decrease for r_1 and r_2 going to infinity. The matrices are diagonalized with the Lanczos algorithm, which is a highly efficient iterative method to obtain few eigenvalues of huge matrices in a short CPU time [14]. Convergence of the results are checked with systematic changes of α and θ. We have thus computed few hundred ${}^1\mathbf{P}^o$ states, which are the only ones populated in one photon experiment starting from the Helium ground state (${}^1\mathbf{S}^e$). The resulting cross-section from below the $N = 2$ up to above the $N = 8$ threshold – the highest energy where experimental spectra are available – is shown in figure 2, convoluted with a lorentzian at the experimental resolution (2 meV for $N = 2, 3$ and 4 meV for $N = 4, 5, 6$) or at a slightly better resolution (1 meV above the $N = 6$ threshold). The agreement with the figures from references [10,12] is excellent, emphasizing the efficiency of our calculations. The theoretical positions, linewidths and Fano-q parameters are in good agreement with previous works [8,10].

Below the $N = 2$ (resp. $N = 3$), three (resp. five) different series are clearly distinguishable, either by their widths (see fig. 1) or by the expectation value of $\cos\theta_{12}$, as shown in Fig. 3, where the real part of $-N\cos\theta_{12}$ is plotted (the imaginary part is at least ten times smaller) versus the effective principal quantum number n_{eff} of the outer electron measured from the N^{th} threshold, proving thus the validity of Herrick classification in these energy ranges. Still, the

chaotic aspect of the Helium atom is already observable in the fluctuations of the smallest widths (see Fig. 1) (and also in the Fano-q parameters), which will be amplified at higher energies.

Below the $N = 5$ and $N = 6$ thresholds, irregularities due to the interaction with the $6, 4_6$ (resp. $7, 5_7$) state from the upper series are visible, in perfect agreement with the experimental observation. Below the $N = 7$, $N = 8$ and $N = 9$ thresholds, the computed cross-section – represented at a better resolution – reproduces very well the various overlapping series, with an increasing number of perturbers coming from higher series. Furthermore, we show new peaks that are not yet experimentally resolved – such as the members of the $9, 7_n$ series – but whose observation could be possible with a (slight) increase of the experimental resolution and signal to noise ratio. In this energy range, the various series are so strongly coupled and overlapping that the approximate Herrick classification breaks down [15,16], giving rise to an irregular spectrum, showed by Fig. 1 where no general trend can be easily recognized in the widths of the various resonances. This irregularity is the quantum manifestation of the chaotic classical dynamics. In this regime, the photo-ionization cross-section results from the superposition of various overlapping Fano profiles, eventually leading to random-like fluctuations in the cross-section known as Ericson fluctuations [17]. Predicted around the $N = 30$ threshold in the 1-dimensional helium atom [18], this irregular regime takes place at much lower energy in the real helium atom, because of the increased density of states. The ratio between the linewidth Γ and the local mean level spacing s is displayed in Fig. 4 for the $N = 4$, $N = 6$ and $N = 8$ thresholds. We clearly see that for $N = 8$, a vast majority of resonances lie above the line $\Gamma/s = 1$, corresponding to the overlapping resonances regime. The published experimental results [12], seem to show irregular fluctuations, the first steps towards the Ericson fluctuations.

In conclusion, our results are, as far as we know, the *ab initio* calculations for the double excited $^1\mathbf{P}^o$ states of the helium atom at the highest energy ever done. They are in excellent agreement with the presently available experimental data. Importantly, they show that the strongly irregular regime where various resonances overlap leading to Ericson fluctuations in the photo-ionization cross-section is almost reached experimentally, which opens the way to their experimental observation and more generally to a new generation of experiments probing the chaotic aspects of the helium atom.

During this research, B.G. has been financially supported by a fellowship of the European Commission under contract No. ERBCHBICT941418. CPU time on a Cray C98 computer has been provided by IDRIS. Laboratoire Kastler Brossel is laboratoire de l'Université Pierre et Marie Curie et de l'Ecole Normale Supérieure, unité associée 18 du CNRS.

---

[1] J.W. Cooper, U. Fano and F. Prats, Phys. Rev. Lett. **10**, 518 (1963).
[2] D.R. Herrick and O. Sinanoglu, Phys. Rev. A **11**, 97 (1975).
[3] C.D. Lin, Phys. Rev. A, **29**, 1019 (1984).
[4] J.M. Feagin and J.S. Briggs, Phys. Rev. A **37**, 4599 (1988).
[5] Y.K. Ho, Phys. Rev. A **44**, 4154 (1991).
[6] J.-Z Tang, S. Watanabe and M. Matsuzawa, Phys. Rev. A **48**, 841 (1993).
[7] K. Richter, J.S. Briggs, D. Wintgen and E.A. Solov'ev, J. Phys. B: At. Mol. Opt. Phys. **25**, 3929 (1992).
[8] D. Wintgen and D. Delande, J. Phys. B: At. Mol. Opt. Phys. **26**, L399 (1993).
[9] R.P. Madden and K. Codling, Phys. Rev. Lett. **10**, 516 (1963).
[10] M. Domke, K. Schulz, G. Remmers, G. Kaindl, and D. Wintgen, Phys. Rev. A, **53**, 1424 (1996).
[11] D.M. Brink and G.R. Satchler, *Angular Momentum*, Academic Press (1975).
[12] K. Schulz *et al*, Phys. Rev. Lett. **77**, 3086 (1996).
[13] A. Buchleitner, B. Grémaud and D. Delande, J. Phys. B: At. Mol. Opt. Phys. **27**, 2663 (1994).
[14] T. Ericsson and A. Ruhe, Math. Comp. **35**, 1251 (1980).
[15] A. Bürgers, D. Wintgen and J.M. Rost, J. Phys. B: At. Mol. Opt. Phys. **28**, 3163 (1995).
[16] B. Grémaud and P. Gaspard (to be published).
[17] T. Ericson, Phys. Rev. Lett. **5**, 430 (1960).
[18] R. Blümel Phys. Rev. A, **54**, 5420 (1996).

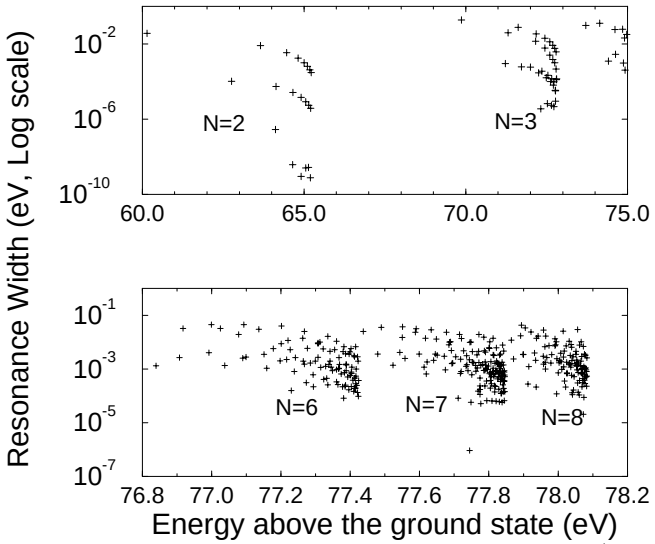

FIG. 1. Positions (in eV above the ground state) and widths (logarithmic scale) of $^1\mathbf{P}^o$ resonances of the Helium atom. The upper plot displays the states below the $N = 2$ and $N = 3$ thresholds, where the various series can be distinguished without ambiguity from their widths, in agreement with Herrick classification of doubly excited states. In the lower plot, displaying the states below the $N = 6, 7, 8$ thresholds, the various series are strongly coupled and overlapping, which is a quantum manifestation of classical chaos in this system.

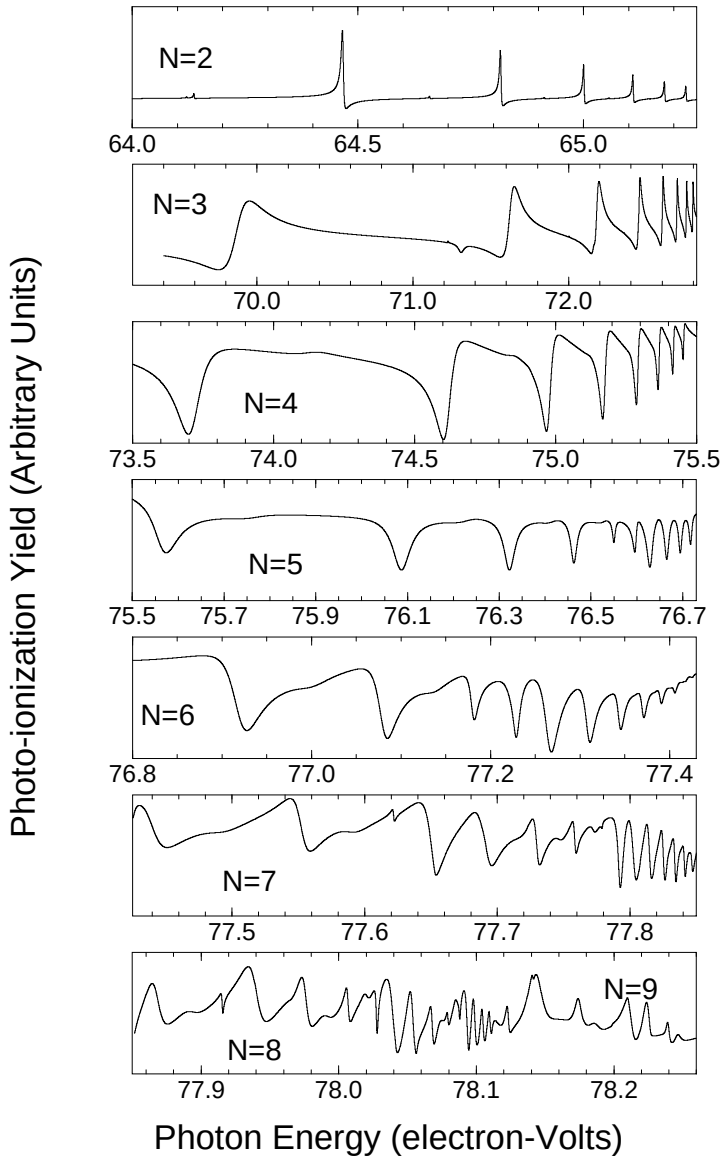

FIG. 2. Calculated photo-ionization cross-section of the helium atom from the $N = 2$ (upper plot) to the $N = 8$ and 9 (lower plot) series. The raw spectrum has been convoluted by a lorentzian of width 2 meV for $N = 2, 3$ and 4 meV for $N = 4, 5, 6$ (equal to the experimental resolution) and 1 meV for $N = 7, 8, 9$. The calculated cross-section is in excellent agreement with the experimental results of references [10,12], displaying for $N = 7, 8, 9$ new peaks, not yet experimentally observed. At the highest energies, the various series overlap strongly, leading to irregular fluctuations of the cross-section and breakdown of the classification. Only the fluctuating part of the cross-section is here represented, the smooth background being subtracted.

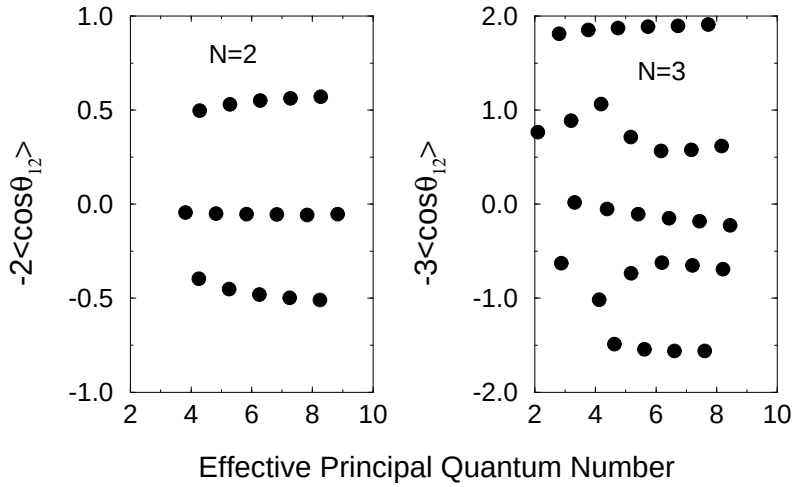

FIG. 3. Real part of the expectation values of $-N\cos\theta_{12}$ for the various resonances below the $N = 2$ and $N = 3$ thresholds. As expected from the Herrick classification scheme of doubly excited states, the value is almost constant across a series, although it slightly differs from the predicted value $-(N-1) \leq K \leq (N-1)$. At higher energy, this classification breaks down.

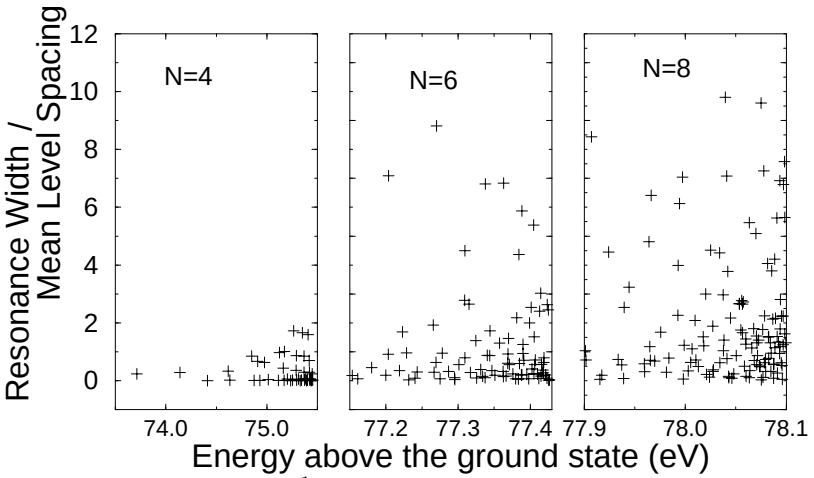

FIG. 4. Ratio between the widths Γ of the various $^1\mathbf{P}^o$ resonances of the helium atom and the local mean level spacing s, displayed for the $N = 4$, $N = 6$ and $N = 8$ thresholds (from left to right). The transition between the regime of well separated resonances to the strong overlapping resonances regime is observed. For higher thresholds, the number of resonances lying above the $\Gamma = s$ line will increase, leading to the observation of Ericson fluctuations in the photo-ionization cross-section.